2015-03-01

An Investigation of Friction Stir Welding Parameter Effects on Post Weld Mechanical Properties in 7075 AA

Steven B. Dickson
Brigham Young University - Provo

An Investigation of Friction Stir Welding Parameter Effects on Post Weld Mechanical Properties in 7075 AA

Steven B. Dickson

A thesis submitted to the faculty of
Brigham Young University
in partial fulfillment of the requirements for the degree of

Master of Science

Tracy W. Nelson, Chair
Carl D. Sorensen
Michael P. Miles

Department of Mechanical Engineering

Brigham Young University

March 2015

ABSTRACT

An Investigation of Friction Stir Welding Parameter Effects on Post Weld Mechanical Properties in 7075 AA

Steven B. Dickson
Department of Mechanical Engineering, BYU
Master of Science

The effects of weld temperature, travel speed, and backing plate thermal diffusivity on the mechanical properties of a weld have been studied. A face centered cubic experiment of design was completed in which the response variables were yield strength, minimum hardness in the HAZ, and charpy impact toughness. Three models were created from the data gathered using a stepwise regression in order to see the effects of each parameter. For the yield strength and minimum hardness it was found that only travel speed and backing plate thermal diffusivities were statistically significant to the properties. The charpy impact toughness saw that all three parameters were statistically significant to its value. In all three models the travel speed had the greatest affect on the material properties.

Keywords: friction stir weldiing, 7075 aluminum, parameter effects analysis, yield strength, minimum hardness, charpy impact test,

ACKNOWLEDGMENTS

I would like to thank everyone that helped me complete this research either directly or through constant encouragement and support. I would especially like to thank my wife, Katelyn Dickson, that would not let me give up even when at times I wanted to. Lastly I would like to thank my advisor, Dr. Tracy Nelson, for giving me the opportunity to do research and help me become a better critical thinker and writer.

This work was performed as part of the National Science Foundation's Center for Friction Stir Processing. The authors gratefully acknowledge the support of NSF and the industrial sponsors of the center.

TABLE OF CONTENTS

LIST OF TABLES

LIST OF FIGURES

CHAPTER 1. INTRODUCTION

Friction Stir Welding (FSW) is a technology that was developed by The Welding Institute in 1991 [1]. Since its discovery the use of FSW has been widely adopted in the welding of aluminum structures including ferry decks and fuel/oxidizer tanks for space launch vehicles. FSW is often used because of its good strength and ductility along with minimizing residual stress and distortion of the base material. These characteristics of FSW are typically attributed to the solid state nature of the process and low energy input to the weldment.

In the early development of FSW most processes were done using modified machine tools such as milling machines. Due to the wide variety of tools in industry it was hard to quantify what system and controllable machine parameters had the largest effect on the mechanical properties of the weld. With the advancement of FSW equipment, the ability to quantify the effects of process variables has increased.

In recent years the Friction Stir Research Laboratory at BYU has developed tools and processes that have been instrumental in advancing the technology in FSW. One of the more recent developments has included the ability to control the peak temperature throughout a weld [2]. By embedding a thermocouple in the pin of the tool the FSW machine can read the temperature of the tool. Using the complex algorithms developed, the computer can then command power to regulate the temperature of the weld. Prior to this technology researchers would record peak temperatures at one location of the weld, but were unable to control that peak temperature through out the weld.

By using the temperature controlled algorithm, FSW researchers can continue to further develop models that will show the sensitivities of various process variables to material properties of the weld. The work presented in this thesis was done to further understand which parameters have the greatest effect on mechanical properties of FSW 7075-T7531 aluminum alloy.

CHAPTER 2. LITERATURE REVIEW

2.1 7075-T7531 Aluminum

Of the 7XXX series aluminum 7075 is one of the most commonly used alloys. This alloy is used frequently because of its advantageous mechanical properties in comparison to other aluminum alloys. The chemical properties of this alloy are listed in table 2.1.

Table 2.1: Chemical composition for 7075 aluminum alloy

Element	Zn	Mg	Cu	Si	Fe	Mn	Cr	Ti	Others
wt%	5.1-6.1	2.1-2.9	1.2-2.0	0.40	0.50	0.30	0.18-0.28	0.20	0.15

2.2 Strengthening Mechanisms of 7075 Al

The mechanisms by which a 7XXX series aluminum gains its mechanical properties are through grain boundary strengthening and precipitation hardening. While these methods affect the strength, research in FSW has shown that precipitation hardening is the primary factor in determining the mechanical properties, such as yield strength, in a 7XXX series aluminum [3]. Grain boundary strengthening has been found to affect the fracture toughness [4].

Precipitation hardening, also known as age hardening, begins when the aluminum alloy brought to a temperature above the solvus and then quenched to room temperature resulting in a super saturated solid solution (SSSS). During the quench, regions known as vacancy rich clusters (VRC) are formed in the microstructure and act as the location for precipitation hardening to occur [5–8]. The concentration of VRCs found in the material matrix is controlled by the quench rate [9]. The path in precipitation hardening occurs is as follows:

$$SSSS \rightarrow VRC \rightarrow GPzones \rightarrow \eta' \rightarrow \eta$$

From the VRCs the Guinier-Preston (GP) zones form followed by the η' precipitates. The η' precipitate is what gives strength to the alloy, and as the alloy is aged the density of these precipitates increase until the alloy reaches a peak strength [10]. If the alloy continues to age then the η' will begin to dissolve into η precipitates. These η precipitates don't contribute as much strength the materials matrix as does the η' precipitates.

The process of precipitation strengthening is highly dependent on the temperature and time. There are two methods for age hardening a material that has undergone a SSSS treatment. The first is known as natural aging, and occurs at room temperature. This method requires the material to age for long periods of times in order to reach its peak strength. Some studies have shown that the natural aging never stops and the material will eventually reach its peak strength and remain there [11]. The second method is an artificial aging treatment of the material. This is done by placing the material in a furnace at an elevated temperature. Typical temperatures for an artificial range is from 130 °C to 180 °C. By doing an artificial aging treatment the material will gain its peak strength much faster. Once its reached its peak strength if the material remains at the elevated it will begin to over age, forming η precipitates, and loose strength.

In FSW it is seen that the weld nugget undergoes a SSSS heat treatment while the heat affected zone (HAZ) typically is affected by the over aging of η' precipitates. By undergoing this thermal cycle the weld nugget can regain most of its strength by doing a post-weld heat treatment while the HAZ is left in its deleterious state.

2.3 Previous FSW Parameter Studies

Throughout the literature many authors have studied the effects of FSW on different mechanical properties by altering either one or two welding parameters at one or two levels [12–14]. Studying only two levels can have inconclusive results because the effect of the parameter might be of a quadratic nature [15]. The most common parameters to vary in the literature is that of travel speed and rotational rate as they are the easiest to control. This section will attempt to compile the previous work that has been done and recognizing that there is a gap in all of the research in that none of them are all inclusive of the welding parameters.

Sato et al. [16] studied how the tool rotational rate (RPM) effects the microstructure and hardness of the weld. Sato concluded that RPM affected the grain size but not the microhardness

of the weld. It was reported that during the welding procedure an increase in peak temperature was observed with increasing RPM. Therefore, the grain growth was attributed to the increase in peak temperature. The difference in microhardness between the welds studied was insignificant and therefore no conclusions were made relating RPM to mechanical properties.

Upadhyay et al. [17, 18] investigated the effects of backing plate thermal diffusivity and travel speed on the hardness of the welds. The author also published a very similar article trying to correlate the axial force to weld properties. In the first article the author concluded that the thermal diffusivity of the backing plate had the greatest effect while the second article attributes it to the axial force.

Hassan et. al [19] did an studied the effects of travel speed and tool rotational rates in 7010 aluminum. They observed that the weld peak temperature increased with increasing tool rotational speed. They also observed that the thermal cycle was the dominant factor in controlling the microstructure of the weld and its accompaning mechanical properties. At high travel speeds they found that the material had higher strength than at lower travel speeds. This was due to the exhibit of higher solute concentrations throughout the weld than those welds run at lower travel speeds. When welds were run at lower travel speeds the heat input becomes excessive allowing for reprecipitation to occur during cooling. This article concludes that travel speed will play an effect on the thermal cycle and therefore control the weld properties.

Cavaliere et al [20] did a study on the effects of travel speed on yield strength in 6082 aluminum. They found that as the travel speed increased the yield strength initially increase (from 40-115 $^{mm}/_{min}$) and then steadily decreased as it approached 460 $^{mm}/_{min}$. The tensile tests in this study were done perpendicular to the weld and therefore saw failure in the heat affected zone. The study believes that this phenominom occurs because at higher travel speeds the material from the advancing side of one weld plate doesn't bond with the mating plate therefore causing voids in the welds.

An analysis done by Elatharasan and Kumar [21] has been one of the more inclusive studies done in that they varied more than two parameters in their study. The study ran 20 welds varying rotational speed, axial load, and traverse speed of the welds while welding in 6061 aluminum. Measuring the yield strength of the weld metal they were able to generate an mathematical model using a response surface methodology. In the analysis it was found that that by increasing the

tool rotational speed and axial force while decreasing the travel speed resulted in an increase of yield strength. While this study has some strength they failed to mention certain essential process parameters used in the study such as tool type and anvil material.

Rajakumar et al. [22] studied the rotational speed, travel speed, axial force, shoulder diameter, and tool hardness as a function of the tensile strength in 6061 aluminum. Their study demonstrated that a response surface methodology can be used to study the effects of individual parameters. The results from this study concluded that the welding speed was the most predominant factor controlling the post-weld mechanical properties. The second factor in determining the mechanical properties was the interaction between the welding speed and the tool rotational rate. In other works, the tool rotational rate has been shown to affect the temperature of the weld in that as rotational speed increase so does the weld temperature [23]. Therefore in the work done by Rajakumar it is unlcear as to whether the effect on mechanical properties seen by to the tool rotational rate was due to the the tool rotating or the peak temperature of the weld.

2.4 Temperature Controlled FSW

While some authors report that the temperature of FSW is relatively constant throughout the weld, none have reported that they have controlled the peak temperature of the weld [24]. Other authors have suggested that the peak temperature of the weld is governed by the travel speed [25].

The Friction Stir Research Lab at Brigham Young University, has developed a method for controlling the peak temperature of a weld by controlling the power of a weld [26]. The tool used for temperature control has a thermal couple embedded into the pin. Using this temperature reading the system them commands power using a PID controller for the desired temperature of the weld. By using this technology a better understanding of how peak temperatures affect weld properties can be investigated.

CHAPTER 3. METHODS

The parameters chosen to investigate for this study were weld temperature, travel speed, and backing plate thermal diffusivity. These parameters were chosen in order to understand which parameter effects the post weld mechanical properties the greatest. In order to find which parameter has the greatest effect on the post weld mechanical properties a design of experiments (DOE) was used to model the effects of each parameter. The mechanical properties tested were all weld metal yield strength, minimum microhardness, and charpy impact fracture toughness.

3.1 Design of Experiments

In order to run a full factorial of levels on 3 factors would require 27 individual welds. It was determined that this would be to time consuming and costly due to all the testing that would be required. Based on the work performed by Hardin and Sloane it was determined that a simpler DOE could be performed with minimal loss in resolution [27]. The DOE that was used in these experiments was a face centered cubic design with only one replicate at the center point which comprises of only 15 individual welds (see appendix A.1 for complete list).

3.1.1 Factors and Levels of DOE

As seen in the background section of this paper, the traverse speed and peak temperature, as it can be correlated to tool rotational speed, are constantly being debated as the primary factors in determining mechanical properties of welds. A third parameter that has not been explored as thoroughly is the backing plate material [28]. In order to use continuous variables for all factors in the study, the thermal diffusivity of the backing plate will be used in evaluating the data. With the recent development of temperature controlled welds it has been decided to use weld temperature as one of the factors in the DOE instead of RPM in order to better understand how the peak temperature effects the post weld mechanical properties. To the authors knowledge, this is one of

Table 3.1: DOE factors and levels

Factor	1	0	-1
Weld Temperature (°C)	425	450	475
Travel Speed ($^{mm}/_{min}$)	50	100	150
Backing Plate	Granite	Al6XN	Steel

the first times that research has been done on mechanical properties using temperature controlled welds. Please refer to table 3.1.1 to see the complete list of all the factors and their accompanying values.

3.2 Weld Setup

All welds in this study were bead on plate welds and were performed on an MTI model RM2 FSW machine using an H13 hardened steel tool with a convex scroll shoulder step spiral (CS4) tool (see appendix A.2 for drawing). Each weld was ran on 9.5 mm thick 7075-T7531 aluminum plates that were 127 mm wide and 1,170 mm long. Welds were ran transverse to the rolling direction of the plate.

3.3 Samples

In order to eliminate the possibility of in-process natural aging, samples were removed at different locations of the weld depending on the travel speed of the weld. This was done to ensure that each sample had roughly the same amount of in-process natural aging prior to removing the plates from the backing plate. Figure A.3 shows a diagram of how samples were removed from a 50 $^{mm}/_{min}$ weld (See appendix A.3 for other diagram).

Once welds were run they were removed from the anvil and placed in the freezer to ensure that minimal natural aging occurred. Careful consideration was taken to ensure that all welds had similar natural aging times prior to placing them in the freezer.

Welds were later removed from the freezer and allowed to reach room temperature prior to being placed in a furnace at 120 °C for 12 hours. This artificial aging treatment was done in order to bring the welds to a stable phase where they would no longer naturally age at room temperature.

3.3.1 Tensile Test

Tensile tests were performed in the longitudinal direction of the weld using all weld material. Three samples were cut from each weld nugget to ensure that only material from the nugget would be used. To see a drawing of the sample size please refer to appendix A.4.

Three samples were tested from each weld using and Instron model 1321 machine at a constant strain rate of 0.1^{-1}. All testing was conducted at a room temperature of approximately 21 °C.

3.3.2 Hardness Testing

In preparation for microhardness samples were polished up through 1 μm diamond polish solution. Vickers micro hardness scans were carried out using 100 gram indents at 300 micron spacing. All tests were trace tests at mid plane of the weld and values reported in the results will be the minimum hardness value found in the heat affected zone (HAZ).

3.3.3 Charpy Testing

Artificially aged samples were prepared for charpy impact testing using ASTM E23-12c standard. All samples were prepared with the notch being placed in the weld nugget. Samples were then tested on a Instron SI-1 series charpy impact testing machine with a hammer weight 30.24 kg and being dropped from a height of 573 mm. Three tests were performed at room temperature and the average of those three were used in evaluating the data.

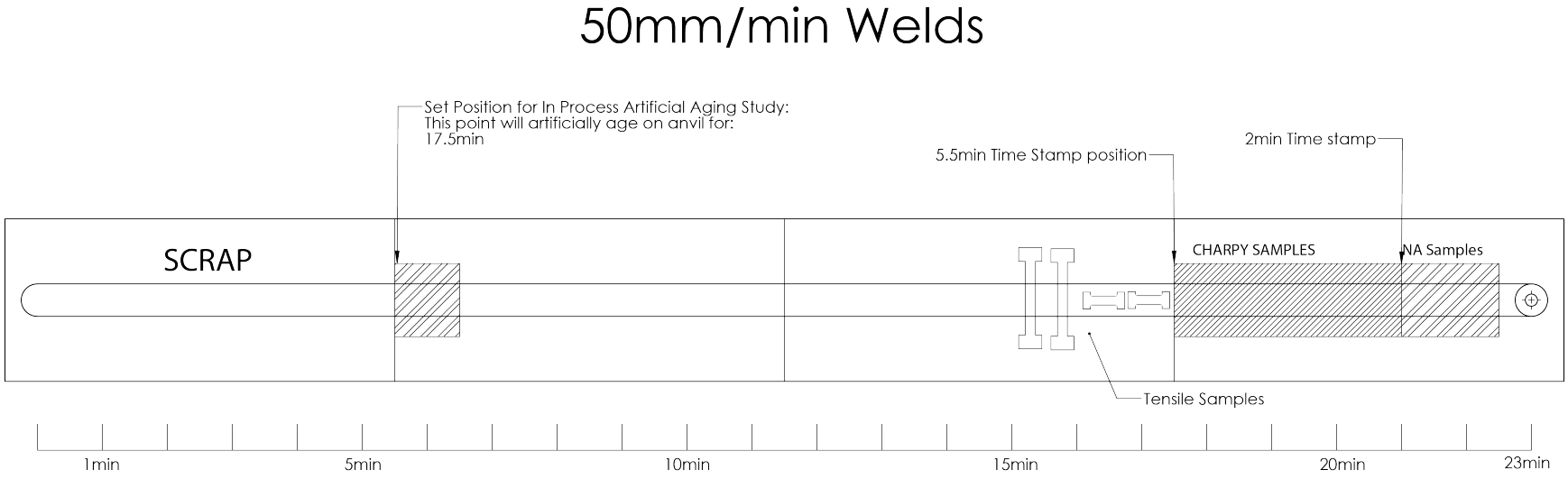

Figure 3.1: Sample removal diagram for welds ran at 50 $^{mm}/_{min}$

CHAPTER 4. ANALYTICAL RESULTS

The data collected from all testing was analyzed using *Jmp* statistical software. A forward step wise regression was done to fit the experimental results to mathematical models. The ending criteria for the regression was a minimum Bayesian information criterion (BIC).

4.1 Yield Strength

Equation 4.1 is the model generated from the regression analysis on the data showing the all weld metal yield strength as a function of the welding parameters. The R^2 and adjusted R^2 values of the model were 0.91 and 0.90 respectively. The equation for the yield strength model is

$$\sigma_y = 249.7 + 1.029x_2 + 3.056x_3 - 0.0116(x_2 - 100)^2 \tag{4.1}$$

where x_2 is the travel speed ($^{mm}/_{min}$), and x_3 is the thermal diffusivity ($^{m^2}/_{s}$), of the backing plate. Figure 4.1 is a graphical representation of equation 4.1 in a three dimensional surface plot.

Using equation 4.1, it was found that the travel speed had the greatest effect on the yield strength of the weld nugget. The yield strength increased by 25% as the travel speed increased while the back plate thermal diffusivity only increased the strength by 10% with increasing values. From the regression model it was found that the weld temperature did not have a statistically significant effect on the yield strength of the nugget.

Studies done previously have shown that both the travel speed and backing plate can affect the microstructure and post-weld mechanical properties [29]. The work done by Rose [30] showed that the backing plate had the greatest affect on the microhardness in HSLA 65. The present work argues that the travel speed had the greatest effect on the post weld mechanical properties. While both studies were done at similar travel speeds and backing plate, the fundamental difference is found in the weld material.

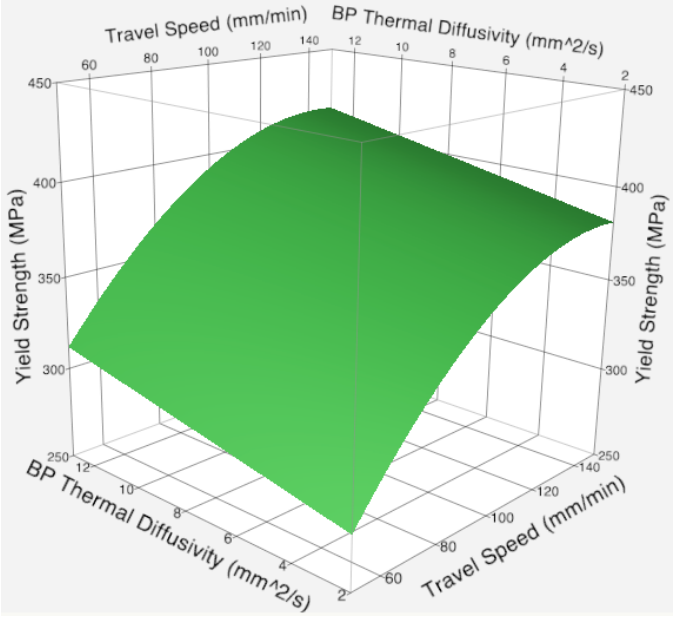

Figure 4.1: Surface plot using the yield strength model shown in equation 4.1

4.1.1 Heat Transfer

As mentioned in the previous section, travel speed and backing plate were the two factors that were statistically significant in determining the yield strength and the minimum hardness of the welds. While both were statistically significant, travel speed had a larger effect on the mechanical properties. With both these parameters having a significant effect on cooling rate [31, 32], an understanding as to why the travel speed had a greater affect is found by doing a simple one dimensional transient heat flow analysis. Previous work in the FSW of HSLA-65 showed that the backing plate had an dominant affect on the mechanical properties, this analysis will compare the 7075 aluminum welds from this study to that of welds in HSLA-65 from a previous study [30].

The thermal conductivity of an 7075 aluminum plate is nearly 5 times greater than that of HSLA-65 steel. Therefore it is hypothesized that the ratio of energy going into the weld plate verse the backing plate is far greater in aluminum than that in steel.

The basic equation for a 1-D transient heat flow problem in a semi-infinite body is

$$q = \frac{kA(T_o - T_i)}{\sqrt{\pi \alpha t}} \tag{4.2}$$

where k is the thermal conductivity of the material, A is the area in which heat is being transferred through, T_i is the initial temperature, T_o is the peak temperature, α is the thermal diffusivity, and t is time. In order to compare the steel welds to the aluminum welds, a comparison will be made on the ratio of heat flow through the welding plate over the heat flow through the backing plate. Figure 4.2 shows the directions in which the calculations will be done.

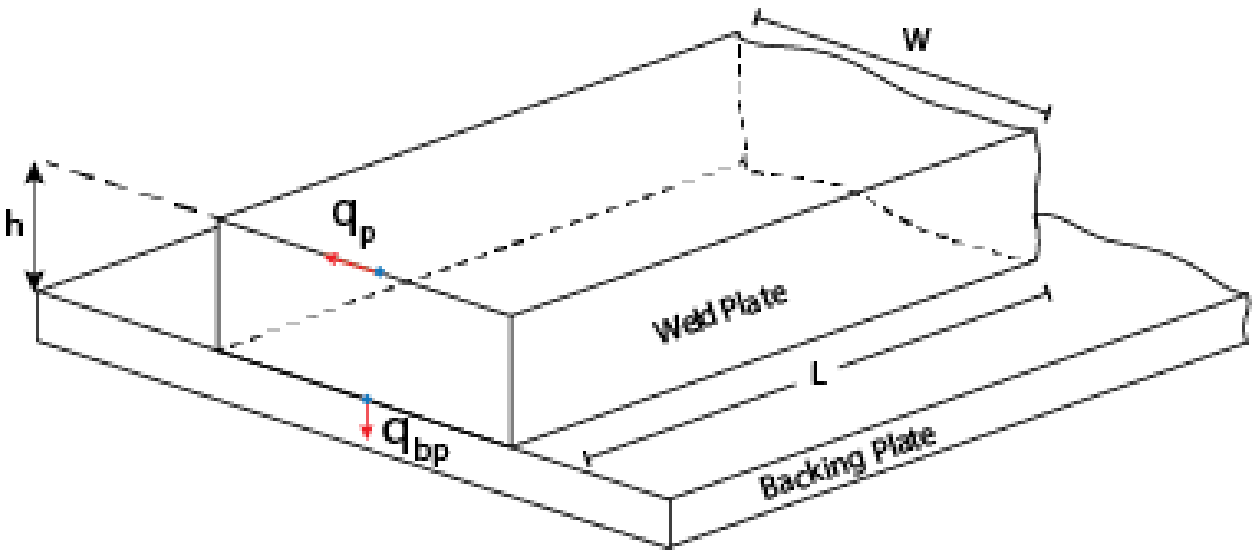

Figure 4.2: Heat flow diagram for a one dimensional analysis

Applying equation 4.2 to the heat flow into the welding plate, q_p, and the into the backing plate, q_{bp}, result in equations

$$q_p = \frac{2(Lh)k_p(T_o - T_i)}{\sqrt{\pi\alpha_p t}} \tag{4.3}$$

$$q_{bp} = \frac{(WL)k_{bp}(T_o - T_i)}{\sqrt{\pi\alpha_{bp} t}} \tag{4.4}$$

where the L, W and h variables correspond to the geometry shown in figure 4.2. All other variables are as explained previously with respect to their material.

Taking the ratio of q_p and q_{bp} results in the cancellation of the length, the temperature difference, and time and gives the resulting equation 4.5

$$\frac{q_p}{q_{bp}} = (\frac{2h}{W})(\frac{k_p}{k_{bp}})(\frac{\alpha_p}{\alpha_{bp}}) \tag{4.5}$$

The values shown in table 4.1 were used to evaluate the ratios for welds done in aluminum and steel. This analysis was done for each of the backing plates that were used in this study and the results can be seen in table 4.2.

Table 4.1: Values used in evaluating the ratio of heat flow from equation 4.5

Material	h(mm)	W(mm)	$k(^W/_{mK})$	$\alpha(^{m^2}/_s)$
Weld Plate				
7075-Al	8.25	127	173	6.4E-5
HSLA	8.25	127	35	9.7E-6
Backing Plate				
Granite	-	-	1.2	2.2E-6
ALX6N	-	-	11.8	2.9E-6
Steel	-	-	50.2	1.3E-5

Table 4.2: The ratio of $^{q_p}/_{q_{bp}}$ for each backing plate ran in this experiment and previous experiments.

	Weld Plate Material	
Backing Plate	Aluminum	Steel
Granite	3.5	1.8
ALX6N	0.4	0.2
Steel	0.2	0.1

With the ratios of the steel welds being half of the aluminum welds it is concluded that twice the amount of energy goes into the backing plate of a steel weld compared to an aluminum weld.

When welding in materials with high thermal conductivity and high thermal diffusivity more heat is lost in the welding plate than in the backing plate. Therefore, the backing plate can be

neglected and the Rosenthal equation can be applied. This equation demonstrates that as the travel speed increases the temperature gradient will decrease thus allowing for higher heat loss [33].

4.2 Minimum HAZ Hardness

Data from micro-hardness was analyzed to find the minimum in each weld. Using this as a response variable the stepwise regression model showed that only the travel speed and thermal diffusivity had an significant effect on the post-weld mechanical properties. Equation 4.6 is the model found in the regression and had an R^2 and an adjusted R^2 value of 0.80 and 0.74 respectively. The variables in the model are the same as those found in equation 4.1.

$$MHV = 86.3 + .13x_2 + .433x_3 - .0008(x_2 - 100)^2 \tag{4.6}$$

Figure 4.3 shows how the travel speed and backing plate thermal diffusivity affected the minimum HAZ hardness.

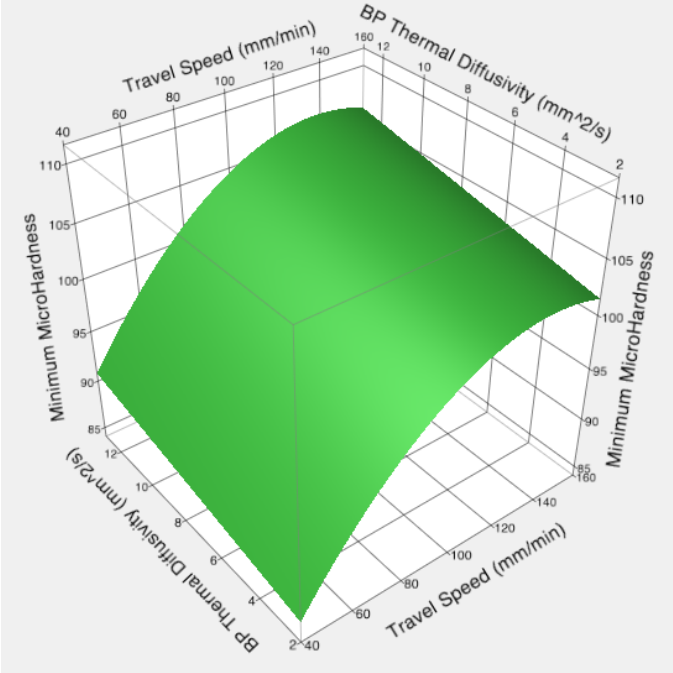

Figure 4.3: Surface plot using of micro-hardness value model shown in equation 4.6

Travel speed had greatest affect on the minimum hardness in the HAZ. It was found that the change in micro-hardness due to the travel speed was on average 12% going from the minimum to maximum values. The change in minimum microhardness due the thermal diffusivity was found to be an average of 4%. The micro-hardness values increased as both travel speed and BP thermal diffusivity increased. These results are consistent with what was seen in the analysis done on yield strength.

4.3 Charpy Impact Energy

The regression analysis for the charpy impact energy showed that all three welding parameters were statistically significant in determining the impact fracture toughness. The equation representing the analysis is shown in 4.7 and had an R^2 and adjusted R^2 value of 0.93 and 0.90 respectively.

$$CVN = 28.28 - .034x_1 - .0616x_2 - .0976x_3 + 0.000858(x_2 - 100)^2 \tag{4.7}$$

x_1 is the weld temperature in degrees Celsius, x_2 is the travel speed in $^{mm}/_{\text{min}}$, and x_3 is the thermal diffusivity of the backing plate in $^{mm^2}/_{\text{sec}}$.

Figure 4.4 shows the surface plots generated from equation 4.7. The parameter that is not displayed in each plot was set to a nominal value. Changing this parameter simply shifted the plots but did not affect the overall geometry of them.

From the graphs presented in figure 4.4 each parameter was evaluated to see how it affected the impact energy of the weld nugget. The impact energy increased by 56% across the travel speed parameters, plot 4.4(a). The weld temperature had the second greatest effect at 24% increase, figure 4.4(c). Finally backing plate had the least significant effect at 13%, figure 4.4(b). In all three cases the impact energy increased as the parameter decreased in value.

It is interesting to note that the temperature had a significant effect on the impact energy toughness but not on the yield strength. This is believed to be because temperature will affect the amount of grain growth, and grain size affects the toughness of this material [4].

Ultimately what effects the post weld mechanical properties of a weld material is the heat flow into a weld plate and the heat flow out of the plate. In the analysis done in this chapter it

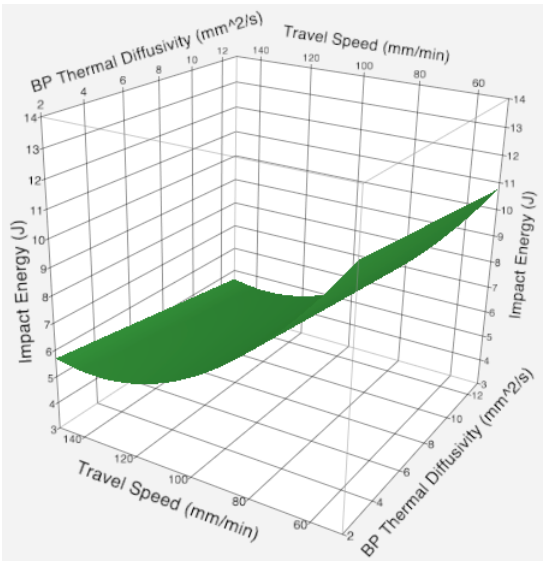

(a)

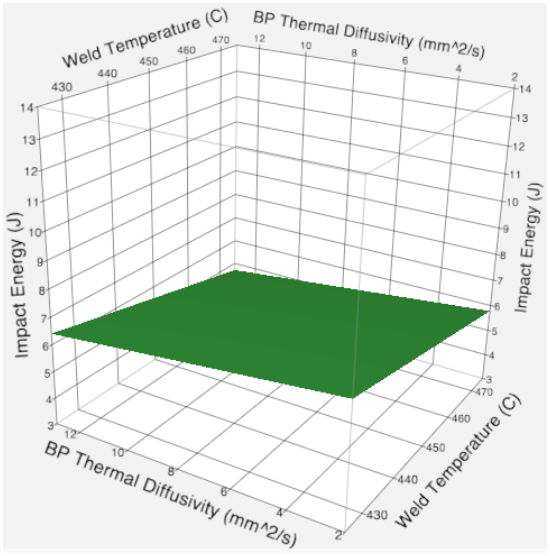

(b)

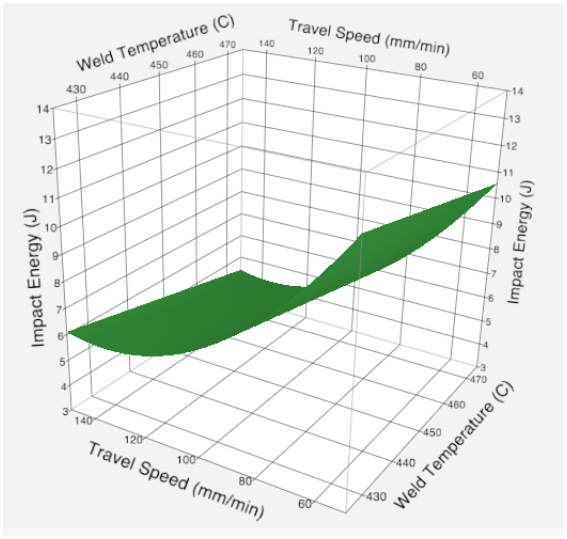

(c)

Figure 4.4: Surface plots of the equation 4.7. (a) Backing plate thermal diffusivity and travel speed as a function of impact energy. (b) Backing plate and weld temperature as a function of impact energy. (c) Travel speed and weld temperature as a function of impact Energy. Parameters not shown in plots were set to nominal values

has been shown that the travel speed is dominate in affecting the post weld mechanical properties. Travel speed is a parameter that will affect the heat input and further discussion of this is found in chapter 5.

CHAPTER 5. DISCUSSION OF RESULTS

5.1 Effects of Heat Input

Comparing the results of this study to other work available in the literature is difficult because of the lack of information presented in the later. The models presented in chapter 4 showed that the controllable machine parameters had a quadratic effect on the post-weld mechanical properties. Due to this quadratic effect it is difficult to compare results to other studies if the same machinine parameters are not used.

The two factors that ultimately change the mechanical properties in FSW are the heat input and the cooling rate. Previous studies [30, 34] it has been seen that the heat input will affect the post-weld mechanical properties linearly. To be able to compare the results across multiple authors work the heat input of a weld must be reported thus allowing for an comparison between studies.

In the present study heat input was calculated by measuring power and controlling the travel speed of each weld. The cooling rate of each weld was not measured and therefore no quantitative reasoning can be made comparing the cooling rate and mechanical properties. Table 5.1 reports the power and heat input for each weld.

Heat input is a calculation of weld power over the travel speed and since the latter was found to be the dominate parameter affecting post weld material properties (see chapter 4) a correlation can be drawn to how the heat input affected the post weld material properties as well.

The yield strength decreased with increasing heat input for each weld and as shown in Figure 5.1. There is a strong linear correlation between the heat input and yield strength for each backing plate. The data is grouped by type of backing plate used for the welds.

The minimum hardness HAZ hardness also decreased with increasing heat input as is seen in Figure 5.2. Similar to the yield strength a strong correlation can be seen between the minimum hardness for each set of backing plates used.

Table 5.1: Power and heat input data for each weld in the current study

Weld	Weld Speed (mm/min)	Power (Watts)	Heat Input (J/mm)
A	150	3200	1270
B	150	2686	1056
C	50	1895	2234
D	50	1679	1980
E	50	2492	2935
F	50	2231	2630
G	150	2604	1023
H	150	2380	935
I	100	2551	1504
J	100	2148	1267
K	150	2880	1134
L	50	2171	2566
M	100	2454	1448
N	100	2066	1219
O	100	2700*	1620*

*Points are estimated due to corrupt files at time of analysis

The impact fracture toughness increased as the heat input increased shown in Figure 5.3. The impact fracture toughness also had a good correlation with the heat input for each weld.

As mentioned previously, the travel speed will affect the heat input of the weld. Looking at Figure 5.4 it is seen that as travel speed increases the heat input decreases non linearly. It is believed that has travel speed continues to increase the heat input will continue to converge.

Figures 5.1 - 5.3 show that as the heat input decreases the post weld mechanical properties tned to converge. This trend is also seen in the models that were generated in chapter 4. Figures 4.1 and 4.3 show that as the travel speed increases (causing the heat input to decrease) the mechanical property plateaus. Therefore, it can be argued that after a given heat input there will be negligible effect in the post-weld mechanical properties due to further increasing heat input.

5.2 Travel Speed vs. Peak Temperature

Reynolds et al. [25] investigated the effects of travel speed and peak temperature on the hardness in the nugget and HAZ of FSW in AA 7050. They reported that both travel speed and peak temperature had a linear affect on the hardness. Peak temperature in this work was not measure

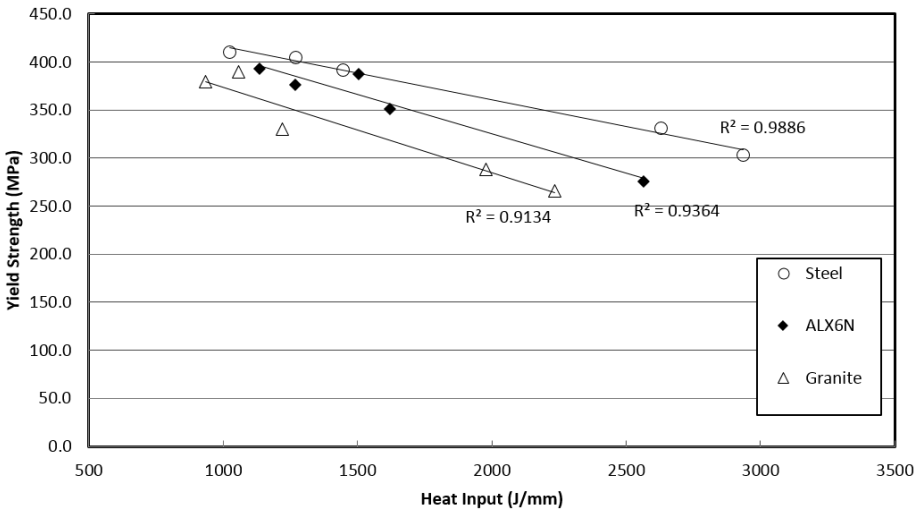

Figure 5.1: All weld metal yield strength as a function of the heat input. Data is grouped by type of backing plate.

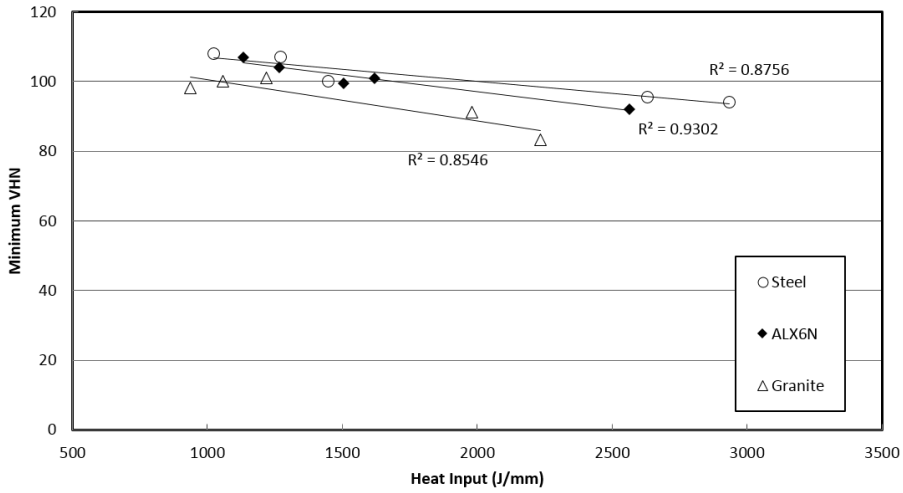

Figure 5.2: Minimum hardness in the HAZ as a function of the heat input. Data is grouped by type of backing plate.

but rather calculated as a function of the power of the machine. Since powers were reported and analysis can be done in comparing his work verse the present work.

Similar to the results presented here, Reynolds showed that the hardness in both the nugget and HAZ increased as the travel speed increased. Figure 5.5 shows how travel speed affected the

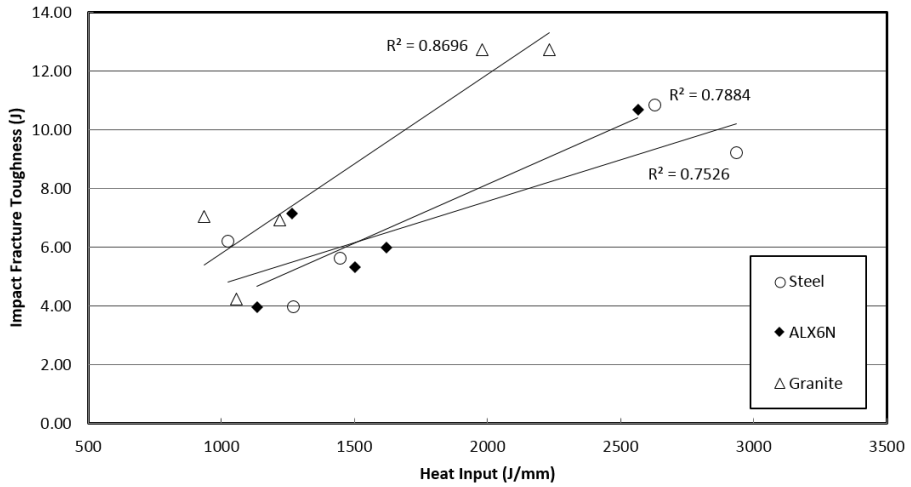

Figure 5.3: Impact fracture toughness as a function of the heat input. Data is grouped by type of backing plate.

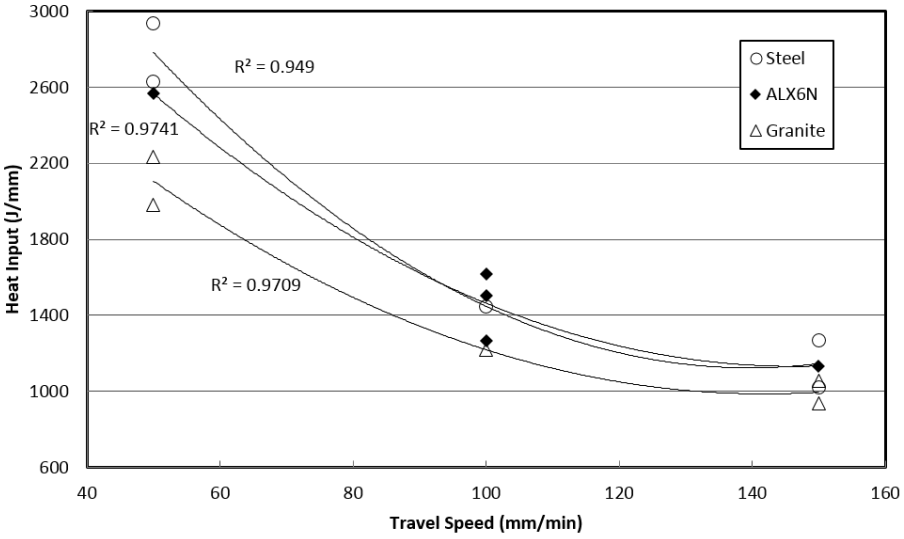

Figure 5.4: Heat input as a function of the travel speed

minimum HAZ hardness in the present work along with the data from Reynolds [25]. This figure shows that there is strong correlation between the travel speed and minimum HAZ hardness despite the differences reported in power and peak temperature. The data compared from this present work and that of Reynolds only represents welds ran using a steel anvil.

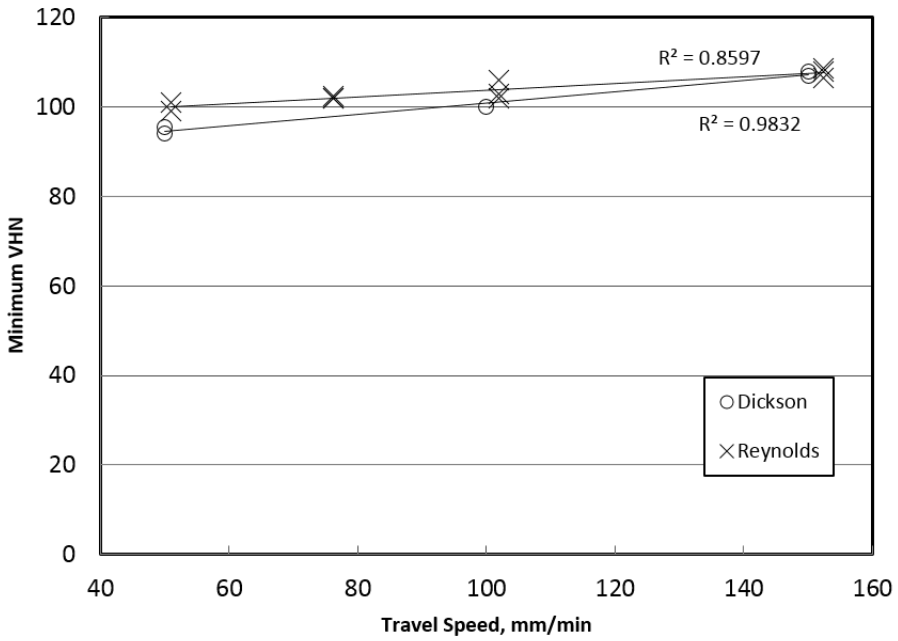

Figure 5.5: Minimum VHN as a function of the travel speed.

Reynolds also reported a correlation between peak temperature and minimum HAZ hardness, but the present work showed no correlation. Figure 5.6 shows the lack of correlation between the weld peak temperature and minimum HAZ hardness.

One explanation as to why there is no correlation between the weld peak temperature and the minimum HAZ hardness is because the HAZ always occurs within a given temperature range. For a 7xxx series aluminum it has been shown that the microstructure in the HAZ is primarily overaged η precipitates [3, 35, 36]. The η phase begins to precipitate at temperatures between 215 and 250 °C [37, 38]. Therefore, regardless of the peak temperature of a weld the minimum HAZ hardness will be determined by the location at which this temperature range occurs.

While the peak temperature does not have a correlation on the value of the HAZ microhardness, the heat input does. Figure 5.7 shows that both the data for Reynolds and the present work have a strong correlation when comparing the heat input to the minimum hardness.

The correlation between the two sets data agrees with the findings of this present work which shows that heat input has a strong correlation to post weld mechanical properties while the peak temperature showed no correlation to the mechanical properties in both studies.

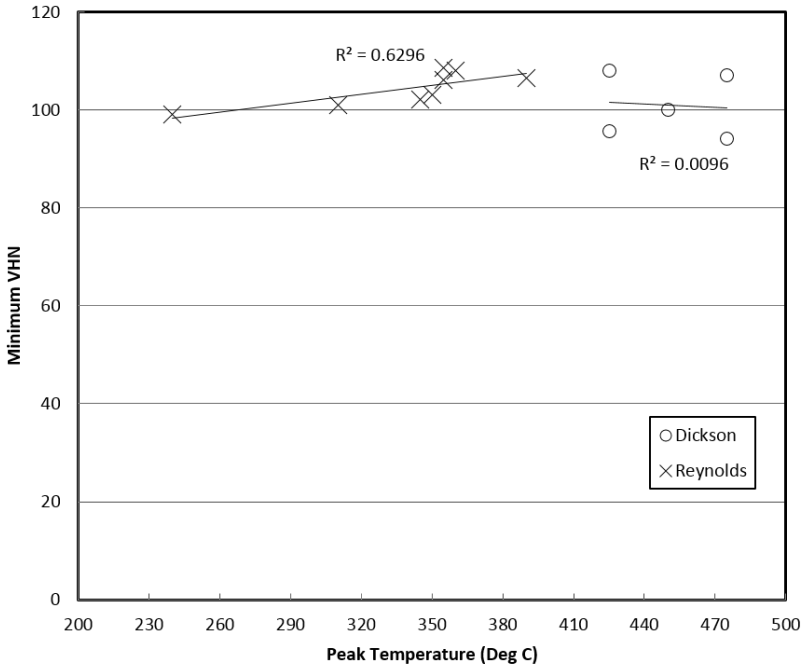

Figure 5.6: Minimum VHN as a function of the peak temperature.

5.3 Multi-factor Parameter Studies

The results from this present study have shown that there is a quadratic correlation between FSW processing parameters and post weld mechanical properties. Therefore, doing studies with only two data points are insufficient for drawing conclusions of the processing parameter effects on post-weld mechanical properties. In order to fully capture the effects of FSW parameters it is important that multiple factors and levels be chosen in order to capture their interactions.

While most literature only alters two parameters, a few researchers have attempted to capture the effects of multiple FSW processing parameters. Recent work by Rajakumar et al. [22] was one of the more thorough studies that has been published on the FSW parameter effects in AA 6061. This study included six factors with five levels each. The parameters studied were tool rotational rate, travel speed, axial force, pin diameter, shoulder diameter, and tool material. A screening effects test was first done to narrow down which factors and levels might have the greatest significance. In total 52 welds were ran with accompanying post weld mechanical property testing. From the results it was found that all 6 factors were statistically significant with the travel

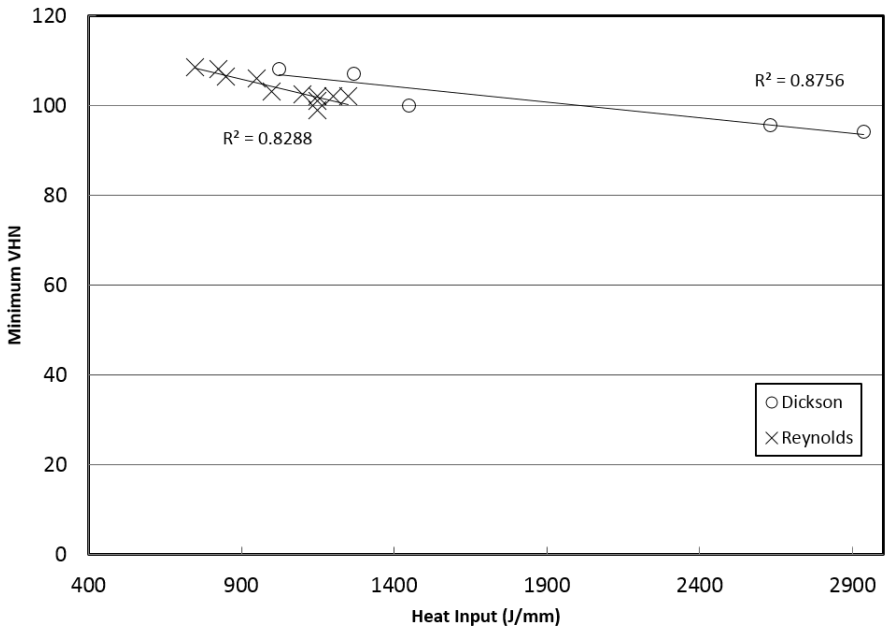

Figure 5.7: Minimum micro hardness as function of heat input for both Reynolds and Dickson data.

speed being the dominate factor. While this research was very thorough, no power or heat inputs were reported and therefore it is difficult to compare the present work to this work.

Other work done by Elatharasan [21] and Lakshminarayanan [39] studied the effects of axial force, tool rotational rate, and travel speed on post-weld mechanical properties in 6XXX series aluminum. While both authors ran welds in similar parameter ranges Lakshminarayanan reported that tool rotational rate had the dominate effect on post weld mechanical properties while Elatharasan reported that travel speed the dominate. Since both of these studies report different findings it is difficult to decipher which is accurate. Additionally, a comparison between the two studies can't be made because no power or heat input data was reported in either studies. Therefore, the data from these studies only pertain to their welding setup and can not be compared with other work.

This work and others [30, 34, 40] have shown that the post-weld mechanical properties and heat input have a linear fit. Individual machine parameters have been shown to have a quadratic effect on the heat input [41]. The quadratic nature of the individual machine parameters makes it

difficult to compare studies. Therefore, by reporting power or heat input comparisons can be made across multiple studies.

CHAPTER 6. CONCLUSION

A thorough study has been done on the affects of weld temperature, travel speed, and backing plate thermal diffusivity on the post weld mechanical properties in FSW 7075-T7531 aluminum alloy. A partial 3 factor DOE was carried out in which the response variables were all weld metal yield strength, minimum hardness in the HAZ, and impact fracture toughness. Three mathematical models were created using a stepwise regression in order to see the effects of each parameter. For the yield strength and minimum hardness it was found that only travel speed and backing plate thermal diffusivity were statistically significant to the properties. The impact fracture toughness observed that all three parameters were statistically significant to its value. In all three models the travel speed had the greatest affect on the material properties.

- Yield strength of the material had a 25% increase with increasing travel speed and an 10% increase with increasing backing plate. It was found that the weld temperature did not have a statistically significant effect on this material property.
- Minimum microhardness in the HAZ had a 12% increase with increasing travel speed and an 10% increase with increasing backing plate. Similar to results in the yield strength, weld temperature did not affect this material property.
- Impact fracture toughness has a 56% increase with decreasing travel speed, a 24% increase with decreasing weld temperature, and a 13% increase with decreasing the thermal diffusivity of the backing plate material.
- There is a non-linear relationship between FSW parameters and post weld mechanical properties. Therefore, studies should investigate more than only two data points in order to accurately capture the effect of welding parameter.

- The thermal cycle is what ultimately drives post weld mechanical properties. In this study it was found that the heat input had strong correlation between all post weld mechanical properties.
- Multi-level parameter studies are an effective way to measuring the significance of welding parameters on material properties. However, in order to compare studies across the literature the heat input must be reported. If no heat input is reported then when authors publish conflicting results no conclusions can be made.

REFERENCES

[1] Thomas, W. M., Nicholas, E. D., Needham, J. C., Murch, M. G., Temple-Smith, P., and Dawes, C. J., 1995. Method of operating on a workpiece, Oct. 24 US Patent 5,460,317. 1

[2] Ross, K. A., 2012. "Investigation and implementation of a robust temperature control algorithm for friction stir welding." Master's thesis, Brigham Young University, April. 1

[3] Mahoney, M., Rhodes, C., Flintoff, J., Bingel, W., and Spurling, R., 1998. "Properties of friction-stir-welded 7075 t651 aluminum." *Metallurgical and Materials Transactions A,* **29**(7), pp. 1955–1964. 2, 21

[4] Hahn, G., and Rosenfield, A., 1975. "Metallurgical factors affecting fracture toughness of aluminum alloys." *Metallurgical Transactions A,* **6**(4), pp. 653–668. 2, 15

[5] Deschamps, A., and Bréchet, Y., 1998. "Influence of quench and heating rates on the ageing response of an al–zn–mg–(zr) alloy." *Materials Science and Engineering: A,* **251**(1), pp. 200–207. 2

[6] Werenskiold, J., Deschamps, A., and Bréchet, Y., 2000. "Characterization and modeling of precipitation kinetics in an al–zn–mg alloy." *Materials Science and Engineering: A,* **293**(1), pp. 267–274. 2

[7] Deschamps, A., Livet, F., and Brechet, Y., 1998. "Influence of predeformation on ageing in an al–zn–mg alloy—i. microstructure evolution and mechanical properties." *Acta Materialia,* **47**(1), pp. 281–292. 2

[8] Thompson, D., Subramanya, B., and Levy, S., 1971. "Quench rate effects in al-zn-mg-cu alloys." *Metallurgical Transactions,* **2**(4), pp. 1149–1160. 2

[9] Bray, J., 1990. *ASM Handbook.*, Vol. 2 ASM International,Materials Par, OH. 2

[10] Jata, K., Sankaran, K., and Ruschau, J., 2000. "Friction-stir welding effects on microstructure and fatigue of aluminum alloy 7050-t7451." *Metallurgical and Materials Transactions A,* **31**(9), pp. 2181–2192. 3

[11] Woo, W., Choo, H., Brown, D. W., and Zhili, F., 2007. "Influence of the tool pin and shoulder on microstructure and natural aging kinetics in a friction-stir-processed 6061–t6 aluminum alloy." *Metallurgical and Materials Transactions A,* **38**(1), pp. 69–76. 3

[12] Peel, M., Steuwer, A., Preuss, M., and Withers, P., 2003. "Microstructure, mechanical properties and residual stresses as a function of welding speed in aluminium aa5083 friction stir welds." *Acta materialia,* **51**(16), pp. 4791–4801. 3

[13] Liu, H., Fujii, H., Maeda, M., and Nogi, K., 2003. "Tensile properties and fracture locations of friction-stir-welded joints of 2017-t351 aluminum alloy." *Journal of Materials Processing Technology,* **142**(3), pp. 692–696. 3

[14] Lee, W.-B., Yeon, Y.-M., and Jung, S.-B., 2004. "Mechanical properties related to microstructural variation of 6061 al alloy joints by friction stir welding." *Materials transactions,* **45**(5), pp. 1700–1705. 3

[15] Elangovan, K., Balasubramanian, V., and Babu, S., 2009. "Predicting tensile strength of friction stir welded aa6061 aluminium alloy joints by a mathematical model." *Materials & Design,* **30**(1), pp. 188–193. 3

[16] Sato, Y. S., Urata, M., and Kokawa, H., 2002. "Parameters controlling microstructure and hardness during friction-stir welding of precipitation-hardenable aluminum alloy 6063." *Metallurgical and Materials Transactions A,* **33**(3), pp. 625–635. 3

[17] Upadhyay, P., and Reynolds, A., 2012. "Effect of backing plate thermal property on friction stir welding of 1." In *Thick AA6061," 9th International Friction Stir Welding Symposium, Huntsville, AL, TWI, Published on CD*. 4

[18] Upadhyay, P., and Reynolds, A., 2012. "Effects of forge axis force and backing plate thermal diffusivity on fsw of aa6056." *Materials Science and Engineering: A,* **558**, pp. 394–402. 4

[19] Hassan, K. A., Prangnell, P., Norman, A., Price, D., and Williams, S., 2003. "Effect of welding parameters on nugget zone microstructure and properties in high strength aluminium alloy friction stir welds." *Science and Technology of Welding & Joining,* **8**(4), pp. 257–268. 4

[20] Cavaliere, P., Squillace, A., and Panella, F., 2008. "Effect of welding parameters on mechanical and microstructural properties of aa6082 joints produced by friction stir welding." *Journal of materials processing technology,* **200**(1), pp. 364–372. 4

[21] Elatharasan, G., and Kumar, V. S., 2013. "An experimental analysis and optimization of process parameter on friction stir welding of aa 6061-t6 aluminum alloy using rsm." *Procedia Engineering,* **64**, pp. 1227–1234. 4, 23

[22] Rajakumar, S., Muralidharan, C., and Balasubramanian, V., 2011. "Predicting tensile strength, hardness and corrosion rate of friction stir welded aa6061-t 6 aluminium alloy joints." *Materials; Design,* **32**(5), pp. 2878–2890. 5, 22

[23] Tang, W., Guo, X., McClure, J., Murr, L., and Nunes, A., 1998. "Heat input and temperature distribution in friction stir welding." *Journal of Materials Processing and Manufacturing Science,* **7**, pp. 163–172. 5

[24] Chao, Y. J., Qi, X., and Tang, W., 2003. "Heat transfer in friction stir welding—experimental and numerical studies." *Journal of manufacturing science and engineering,* **125**(1), pp. 138–145. 5

[25] Reynolds, A., Tang, W., Khandkar, Z., Khan, J., and Lindner, K., 2005. "Relationships between weld parameters, hardness distribution and temperature history in alloy 7050 friction stir welds." *Science and Technology of Welding ; Joining,* **10**(2), pp. 190–199. 5, 18, 20

[26] Ross, K. A., 2012. "Investigation and implementation of a robust temperature control algorithm for friction stir welding." Master's thesis, Brigham Young University, April. 5

[27] Hardin, R., and Sloane, N., 1991. "Computer-generated minimal (and larger) response-surface designs:(ii) the cube." *preprint*. 6

[28] Zhang, Z., Li, W., Shen, J., Chao, Y., Li, J., and Ma, Y.-E., 2013. "Effect of backplate diffusivity on microstructure and mechanical properties of friction stir welded joints." *Materials ; Design,* **50**, pp. 551–557. 6

[29] Bradstreet, B., 1969. "Effect of welding conditions on cooling rate and hardness in the heat affected zone." *Welding Journal American Welding Soc*. 10

[30] Rose, S., 2013. "The effect of cooling rate of friction stir welded high strength low alloy steel." Master's thesis, Brigham Young University, July. 10, 11, 17, 23

[31] Nelson, T., Steel, R., and Arbegast, W., 2003. "In situ thermal studies and post-weld mechanical properties of friction stir welds in age hardenable aluminium alloys." *Science and Technology of Welding & Joining,* **8**(4), pp. 283–288. 11

[32] Chen, C., and Kovacevic, R., 2003. "Finite element modeling of friction stir weldingthermal and thermomechanical analysis." *International Journal of Machine Tools and Manufacture,* **43**(13), pp. 1319–1326. 11

[33] Poorhaydari, K., Patchett, B., and Ivey, D., 2005. "Estimation of cooling rate in the welding of plates with intermediate thickness." *Welding Journal,* **84**(10), pp. 149s–155s. 14

[34] Tribe, A., 2012. "Study on the fracture toughness of friction stir welded api x80." Master's thesis, Brigham Young University, December. 17, 23

[35] Su, J.-Q., Nelson, T., Mishra, R., and Mahoney, M., 2003. "Microstructural investigation of friction stir welded 7050-t651 aluminium." *Acta Materialia,* **51**(3), pp. 713–729. 21

[36] Hwang, R., and Chou, C., 1997. "The study on microstructural and mechanical properties of weld heat affected zone of 7075-t651 aluminum alloy." *Scripta materialia,* **38**(2), pp. 215–221. 21

[37] Viana, F., Pinto, A., Santos, H., and Lopes, A., 1999. "Retrogression and re-ageing of 7075 aluminium alloy: microstructural characterization." *Journal of Materials Processing Technology,* **92–93**(0), pp. 54 – 59. 21

[38] Godard, D., Archambault, P., Aeby-Gautier, E., and Lapasset, G., 2002. "Precipitation sequences during quenching of the aa 7010 alloy." *Acta Materialia,* **50**(9), pp. 2319–2329. 21

[39] Lakshminarayanan, A., and Balasubramanian, V., 2008. "Process parameters optimization for friction stir welding of rde-40 aluminium alloy using taguchi technique." *Transactions of Nonferrous Metals Society of China,* **18**(3), pp. 548–554. 23

[40] Wei, L., and Nelson, T. W., 2012. "Influence of heat input on post weld microstructure and mechanical properties of friction stir welded hsla-65 steel." *Materials Science and Engineering: A,* **556**, pp. 51–59. 23

[41] Pew, J. W., Nelson, T., and Sorensen, C., 2007. "Torque based weld power model for friction stir welding." *Science and Technology of Welding; Joining,* **12**(4), pp. 341–347. 23

APPENDIX A. METHODS APPENDIX

A.1 Complete Weld List

This is the complete weld list used in the experiments presented in this thesis

Weld	*Temperature (deg. C)*	*Travel Speed (mm/min)*	*Backing Plate*
A	475	150	Steel
B	425	150	Steel
C	475	150	Granite
D	450	100	AL6XN
E	450	50	AL6XN
F	475	50	Granite
G	425	50	Steel
H	425	100	AL6XN
I	450	100	Granite
G	425	50	Granite
K	450	100	Steel
L	475	50	Steel
M	425	150	Granite
N	450	150	AL6XN
O	475	100	AL6XN

Figure A.1: The complete weld list for the study done in this thesis.

A.2 Tool Drawing

This is the drawing for the tool that was used in this research. This tool was developed by BYU Friction Stir Research Laboratory and is proprietary property.

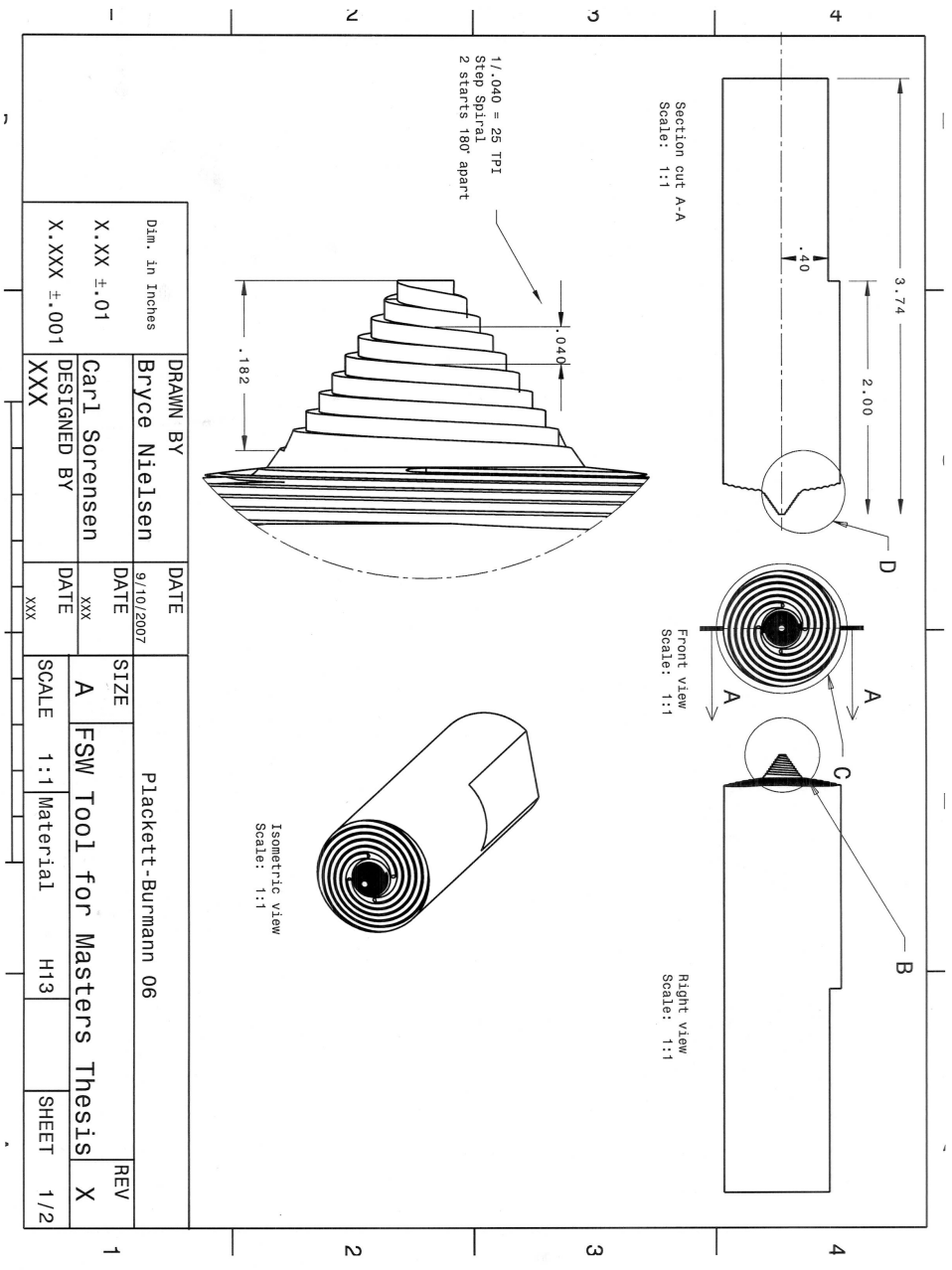

Figure A.2: CS4 Welding tool geometry.

A.3 Weld Cutout Diagrams

This section shows all the weld cutout diagrams that were used for the welds in this study. Each cutout was design based on the travel speed and was done so that all welds had the equivilant amount of time on the anvil prior to removal.

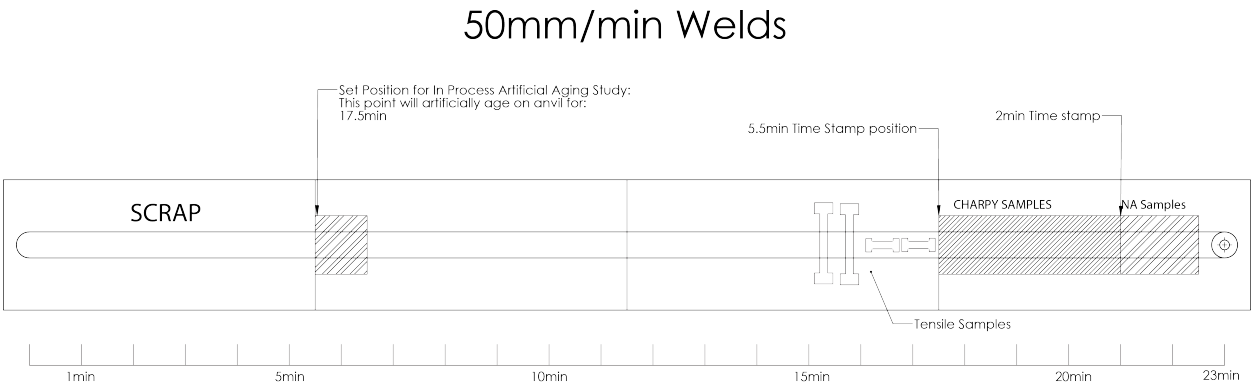

Figure A.3: Sample removal diagram for welds ran at 50 $^{mm}/_{min}$

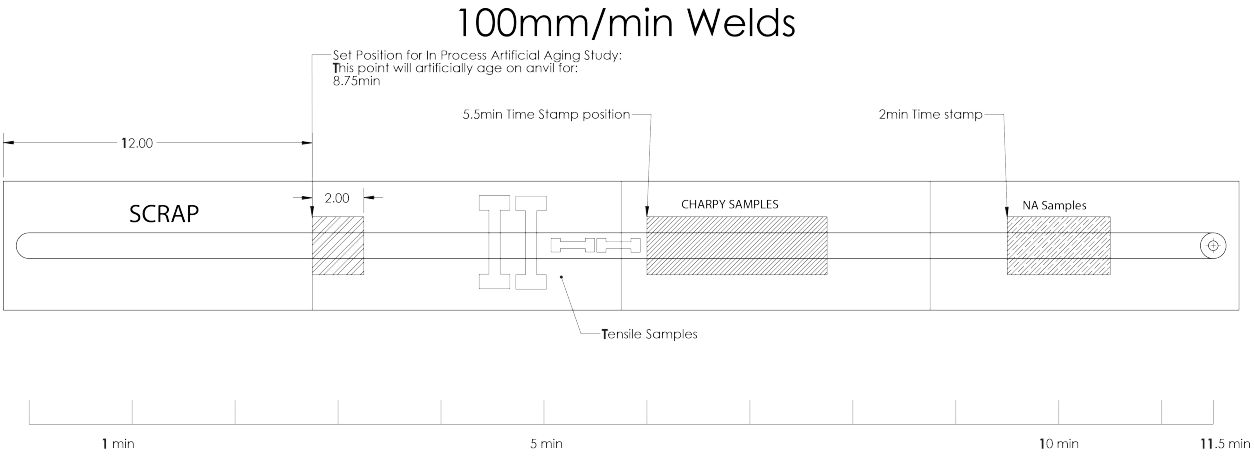

Figure A.4: Sample removal diagram for welds ran at 100 $^{mm}/_{min}$

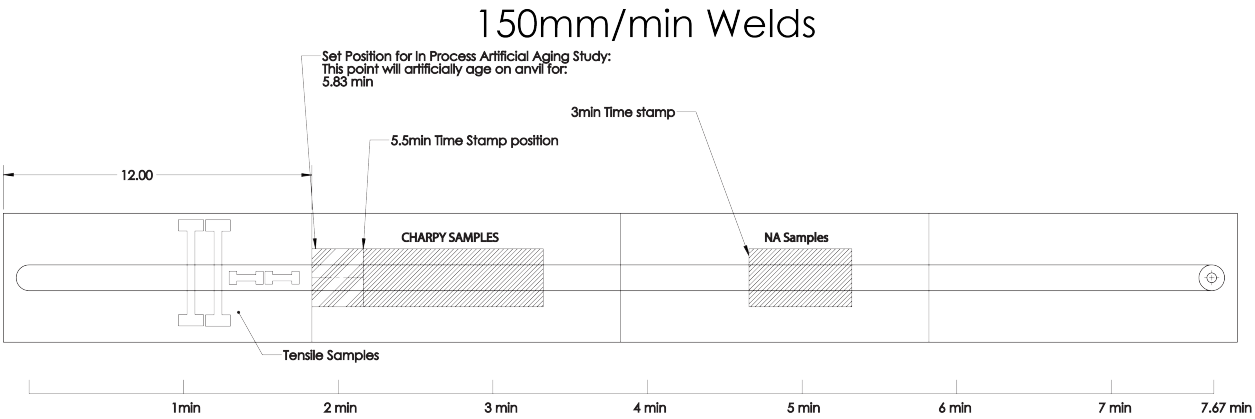

Figure A.5: Sample removal diagram for welds ran at 150 $^{mm}/_{min}$

A.4 Tensile Test Drawing

This drawing was used in machining all tensile sample specimens. All tensile specimens were taken from all weld material.

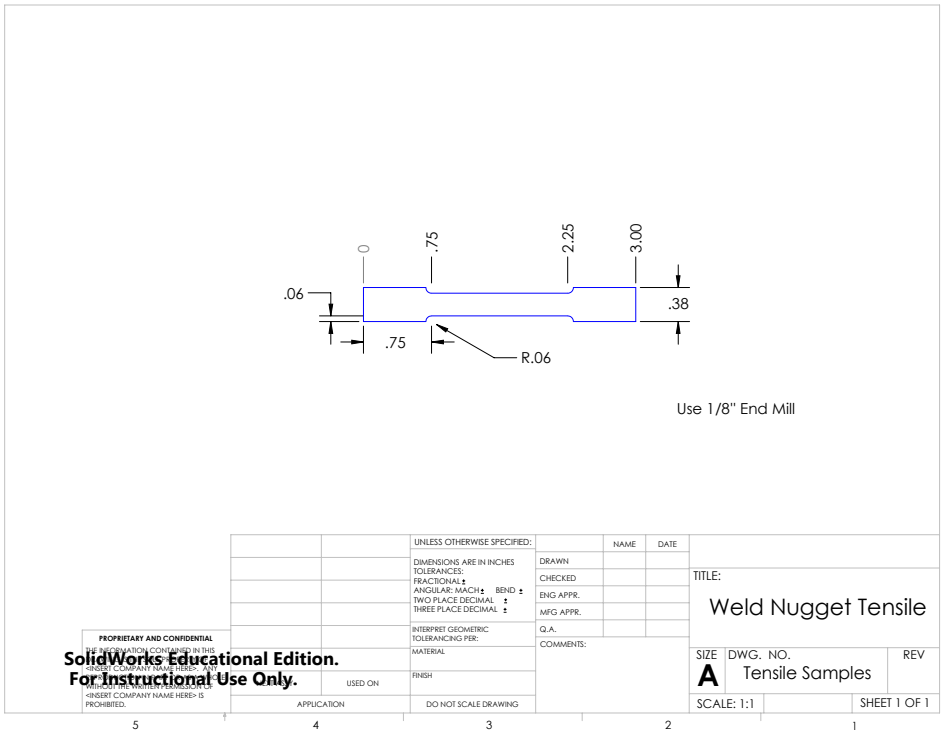

Figure A.6: Tensile sample drawing

APPENDIX B. RESULTS

B.1 Complete Weld Data

This is the complete weld list along with all of the data from the machine and different tests done in the study.

Weld	Temp °C	Weld Speed (mm/min)	Backing Plate Thermal Diffusivity (mm^2/s)	CVN (Joules)	Yield Strength (MPa)	Grain Size (µm)	Vickers MicroHardness (HAZ)	Vickers MicroHardness (Nugget)	Power (Watts)	Heat Input (J/mm)
A	475	150	12.76	3.97	404.9	1.91	107	157.03	3200	1270
B	475	150	2.25	4.24	389.5	1.92	100	147.7	2686	1056
C	475	50	2.25	12.72	266.3	2.4	83.3	118.92	1895	2234
D	425	50	2.25	12.72	288.0	1.67	91.3	117.71	1679	1980
E	475	50	12.76	9.21	302.7	2.01	94.1	133.68	2492	2935
F	425	50	12.76	10.85	331.2	1.69	95.6	127.95	2231	2630
G	425	150	12.76	6.21	409.7	1.15	108	147.92	2604	1023
H	425	150	2.25	7.04	379.3	1.66	98.1	144.48	2380	935
I	475	100	2.93	5.32	387.1	2.03	99.4	140.29	2551	1504
J	425	100	2.93	7.16	376.0	1.66	104	142.14	2148	1267
K	450	150	2.93	3.97	393.0	1.76	107	157.07	2880	1134
L	450	50	2.93	10.67	275.7	2.04	92.1	127.6	2171	2566
M	450	100	12.76	5.62	391.3	1.94	100	149.54	2454	1448
N	450	100	2.25	6.92	330.1	1.78	101	143.69	2066	1219
O	450	100	2.93	5.98	351.4	1.84	101	147.8	-	-

Figure B.1: Complete data set from study